Journal of Virological Methods 264 (2019) 11–17

Contents lists available at ScienceDirect

Journal of Virological Methods

journal homepage: www.elsevier.com/locate/jviromet

Engineering of the hepatitis C virus helicase for enhanced seroreactivity

Christopher C. Marohnic[a,*], Larry G. Birkenmeyer[a], M. Felicia Bogdan[b], Edwin C. Frias[a], Kathy S. Otis[a], Mary Ann P. Palafox[a], Troy D. McSherry[a], Svetoslava D. Gregory[a], Cheng Zhao[a], Robin A. Gutierrez[a], John C. Prostko[a], A. Scott Muerhoff[a]

[a] Abbott Laboratories, Diagnostics Division, Applied Research and Technology, Abbott Park, IL, USA
[b] Abbott Laboratories, Diagnostics Division, Research and Development Process Design, Abbott Park, IL, USA

ARTICLE INFO

Keywords:
Hepatitis C virus
NS3
Helicase
Immunodiagnostic
Seroconversion

ABSTRACT

Hepatitis C Virus c33, a recombinant protein comprising residues 1192–1457 of NS3 helicase, has been a mainstay of HCV serology for decades. With seven unpaired cysteines, seroreactivity of *E. coli* expressed c33 is dependant on reductants. While engineering a c33 replacement for new anti-HCV serological tests, we sought to reduce oxidation sensitivity, a liability for immunodiagnostic reagent stability. A series of cysteine-to-serine substituted variants of a c33-like antigen was constructed and evaluated for reactivity against a panel of HCV-positive sera. Several variants were essentially nonreactive while others exhibited reactivity similar to or better than the wild-type construct. One demonstrated equivalent potency to wild-type but also diminished DTT dependence. To explore enhanced anti-NS3 reactivity, we constructed and examined an expanded series of antigens comprising individual helicase domains, the full-length helicase, additional cysteine-to-serine variants, and variants at positions critical to catalytic activity. Immunoassays using these latter NS3 helicase recombinants demonstrated that domain 1 possessed significantly more seroreactivity than previously believed, that the use of soluble full-length helicase protein enhanced sensitivity by several-fold over c33, and that anti-NS3 helicase seroreactivity was further enhanced by the introduction of point mutations which altered the catalytic activity or oxidation sensitivity of the antigen.

1. Introduction

The hepatitis C virus (HCV) is a positive sense, single-stranded, enveloped RNA virus of the Flaviviridae family and Hepacivirus genus. It was first isolated in 1989 by Choo et al. (Choo et al., 1989) as the primary source of transfusion-associated non-A, non-B type hepatitis (Choo et al., 1990; Kuo et al., 1989). Recent estimates suggest that 130–170 million people worldwide are chronically infected with 3–4 million new infections annually, and that at least 350,000 HCV-induced cases of hepatocellular carcinoma result in death per year (Wise et al., 2008). According to estimates from the U.S. Food and Drug Administration, sustained virologic response to direct-acting antivirals and host-targeting agents has resulted in HCV cure rates exceeding 90% (*Faster, Easier Cures for Hepatitis C*. Available from: http://www.fda.gov/ForConsumers/ConsumerUpdates/ucm405642.htm). Underpinning successful HCV prevention and treatment programs are blood screening and diagnostic assays that protect transfusion recipients, identify acute and chronic infections, and monitor patient response to therapeutic intervention.

Since 1989, several iterations of anti-HCV serological assays have been developed with continuously improving sensitivity to address diagnostic and transfusion demands (Alter et al., 1989; Kleinman et al., 1992; Lee et al., 1995; Lelie et al., 1992). Highly sensitive nucleic acid-based testing (NAT) and core antigen assays can reveal HCV infection in the preseroconversion window period prior to detection of the antibody response (Selvarajah and Busch, 2012). Spanning weeks to months, the preseroconversion window is the predominant hurdle for next generation anti-HCV assays. Cloherty et al. proposed a diagnostic algorithm that maximizes the effectiveness of anti-HCV serological testing in conjunction with NAT and core antigen testing (Cloherty et al., 2016).

Via a single open reading frame, the HCV genome encodes a ~3000 amino acid polyprotein precursor that is co- and post-translationally processed by host and viral proteases into structural (core, E1, E2, and p7) and non-structural proteins (NS2, NS3, NS4A, NS4B, NS5A, and NS5B). First-generation anti-HCV serological tests utilized c100-3, a recombinant antigen comprising viral amino acids 1569–1931 spanning the C-terminus of NS3 and most of NS4, fused to superoxide dismutase (Kuo et al., 1989). Sensitivity was improved with each subsequent

* Corresponding author.
E-mail address: christopher.marohnic@abbott.com (C.C. Marohnic).

https://doi.org/10.1016/j.jviromet.2018.10.019
Received 7 August 2018; Received in revised form 24 October 2018; Accepted 25 October 2018
Available online 28 October 2018
0166-0934/

generation assay utilizing recombinant antigens spanning additional immunoreactive regions of the viral polyprotein.

A number of diagnostic assays have relied on the *E. coli*-produced HC-43 protein, comprising the c33 antigenic region of NS3 (amino acids 1192–1457) tethered to the core antigen (amino acids 1–150) from the HCV Hutchenson strain (i.e., HCV-1; (Ogata et al., 1991)). Expression yielded HC-43 inclusion bodies that were solubilized with urea, reductant, and SDS to obtain pure, monomeric protein (unpublished results). It was determined that the C-terminal 25 amino acids of c33 conferred enhanced reactivity via a discontinuous conformational epitope (Palenzuela et al., 2006). In that study, rNS3 was expressed at 37 °C, extracted from inclusion bodies using 8 M urea, and purified under denaturing conditions.

Finally, others have characterized a series of NS3 helicase recombinant proteins produced in *E. coli* with induction at 30 °C, demonstrating enhanced stability and seroreactivity of NS3 3D (amino acids 1188–1654) (Rebuzzini, 2009). Enhanced performance was attributed to proper protein folding when material was stored in an inorganic buffer. Importantly, the study challenged the notion that the immunodominant epitopes of NS3 were limited to the c33 region.

To optimize seroconversion sensitivity of NS3 helicase antigen in anti-HCV assays without dependence on reducing agents, a series of NS3 helicase variants was iteratively constructed and characterized. With the goal of soluble production of c33, an initial series of mutants was made in which 5 of the 7 native cysteine residues were replaced, singly or in groups, by serine. A second series that added or deleted NS3 helicase globular domains to c33 was constructed to gauge relative contributions to seroreactivity. Finally, a third series of full-length helicase variants was designed with the rationale that mutants known to affect the ATPase and or helicase activities of the enzyme could potentially alter presentation of conformational epitopes that enhance seroreactivity.

2. Materials and methods

2.1. Cloning, expression, and purification of HCV NS3 helicase variants

The nucleotide sequence encoding c33 (amino acids 1192–1457 of HCV-1, extracted from UniProt entry P26664 (UniProt, 2015)) was codon optimized for *E. coli* expression and cloned into a modified pET32a vector wherein the thioredoxin fusion protein and linker was eliminated and replaced with methionine. Amino-terminal residues 1192–1215, derived from the protease region of NS3, were retained due to the presence of an epitope which enabled the use of a well-characterized anti-NS3 monoclonal antibody for capture/detection of the expressed protein. Carboxyl-terminal GSGSG-linker, hexahistidine tag, GG linker, and biotinylation tag (GLNDIFEAQKIEWHE) sequences were included to facilitate IMAC purification and to direct enzyme-mediated biotinylation (Beckett et al., 1999) of the proteins, respectively. The resulting plasmid was designated pET-9NB49H-Cbt and the expressed protein was designated 9NB49H-Cbt.

PCR of colony lysates was employed for screening of *E. coli* XL10-Gold (Agilent) transformants, selected on Luria-Bertani broth (LB)-agar plates supplemented with ampicillin (100 μg/ml). Plasmid DNA was then purified from colonies exhibiting the anticipated PCR band and the DNA sequence of the constructed plasmid was determined with a minimum of 2-fold coverage across the open reading frame using the BigDye Terminator v1.1 Cycle Sequencing Kit (Applied Biosystems), performed according to the manufacturer's protocol, and analyzed on an ABI 3130xl Genetic Analyzer (Applied Biosystems), also according to the manufacturer's protocol. Raw sequence data was aligned to reference and annotated using Sequencher software (Version 5, Gene Codes Corp.). The sequence of the constructed plasmid was confirmed to match the design.

E. coli BL21(DE3) cells were co-transformed with pET-9NB49H-Cbt and pBirAcm (Avidity LLC; encoding *E. coli* biotin ligase). Transformants were then selected on LB-agar plates supplemented with ampicillin (100 μg/ml) and chloramphenicol (10 μg/ml). Protein expression was achieved by culturing the transformed bacteria in terrific broth (TB) medium, supplemented with ampicillin (100 μg/ml) and chloramphenicol (10 μg/ml). Cells were grown in shake flasks at 37 °C to an OD600 nm of ~0.5 and then cooled to 25 °C for 30 min prior to induction with 1 mM IPTG for an additional 18 h. 50 μM biotin was added to the culture at the time of induction. Cells were harvested by centrifugation, and suspended in lysis buffer (50 mM potassium phosphate, 300 mM potassium chloride, 5 mM Imidazole, pH 8.0) supplemented with protease inhibitors. The cell suspension was frozen and thawed, benzonase was added, and the cells were lysed by sonication on ice. To promote site-specific biotinylation, ATP and biotin were added to the lysed cells (3 mM and 0.25 mM final concentrations, respectively) and incubated at room temperature for 2 h. The lysate was divided into soluble and insoluble fractions by centrifugation. IMAC purification was performed on the soluble fraction of the lysate using the Biorad Native IMAC Buffer Kit and Profinity IMAC cartridge (Hercules, CA) according to the manufacturer's instructions. Buffer exchange of the purified protein into PBS pH 7.2 was accomplished by a desalting column or by dialysis. In some instances, HPLC size exclusion chromatography (SEC) using a Tosoh (Tokyo, Japan) G3000SW^{XL} column was applied as a secondary purification step, in which case, only monomeric protein was collected. All buffers used throughout the purification procedure contained 1 mM beta-mercaptoethanol (*B*ME).

The nucleotide sequence encoding 9NB49H-Cbt was site-specifically modified via PCR-mediated mutagenesis to substitute selected cysteine codons with serine codons. Positions mutated are described in Table 1, wherein codon (amino acid) number of the HCV polyprotein sequence is based on that described by Kuiken et al. (Kuiken et al., 2006). DNA sequence confirmation, protein expression, and purification were performed as described above for 9NB49H-Cbt.

Based on helicase domain boundaries suggested by the crystal structure published by Cho et al. (PDB = 8OHM, (Cho et al., 1998)) a series of domain addition/deletion variants was constructed as detailed in Table 2 and as diagramed in Fig. 1. pET-9NB49H-Cbt was used as the plasmid template into which the modified helicase encoding insert sequences were subcloned by Gibson Assembly (Gibson et al., 2009) using a kit from New England BioLabs according to the manufacturer's recommended protocol. Each construct retained the sequences encoding the N-terminal NS3 protease (amino acids 1192–1215), C-terminal GSGSG-linker, hexahistidine tag, GG linker, and biotinylation tag. DNA sequence confirmation, protein expression, and purification were performed as described above for 9NB49H-Cbt.

An additional series of full-length NS3 helicase variants was designed and constructed by site-directed mutagenesis of the pET-NS3h-Cbt plasmid as detailed in Table 3. Note that two variants (the double mutant H129A + R300A and the triple mutant C3S + C5S + P66Q) were obtained by introduction of unintended mutations by PCR error. DNA sequence confirmation, protein expression, and purification were as described above for 9NB49H-Cbt.

Table 1
HCV NS3 (9NB49H or c33) cysteine-to-serine mutants.

Position in HCV polyprotein	Position in NS3	Cys → Ser variant designation
C1305	C279	9NB49H(C1S)-Cbt
C1315	C289	9NB49H (C2S)-Cbt
C1318	C292	9NB49H (C3S)-Cbt
C1394	C368	9NB49H (C4S)-Cbt
C1400	C374	9NB49H (C5S)-Cbt
C1305, C1315, C1318	C279, C289, C292	9NB49H (C1-3S)-Cbt
C1394, C1400	C368, C374	9NB49H (C4-5S)-Cbt
C1305, C1315, C1318, C1394, C1400	C279, C289, C292, C368, C374	9NB49H (C1-5S)-Cbt

Table 2
HCV NS3 helicase domain addition/deletion constructs.

Region(s) of HCV polyprotein expressed	Corresponding region(s) of NS3	Protein designation
1192-1353	166-327	NS3h(d1)
1192-1215 + 1357-1457	166-189 + 331-431	NS3h(d2)
1192-1215 + 1512-1658	166-189 + 486-632	NS3h(d3)*
1192-1215 + 1357-1510	166-189 + 331-483	NS3h(d2ext)
1192-1215 + 1357-1658	166-189 + 331-632	NS3h (d2d3)*
1192-1510	166-483	NS3h (d1d2ext)
1192-1658	166-632	NS3h (helicase)
1192-1215 + 1458-1658	166-189 + 432-632	NS3h(extd3)*

* Protein was not expressed in soluble form.

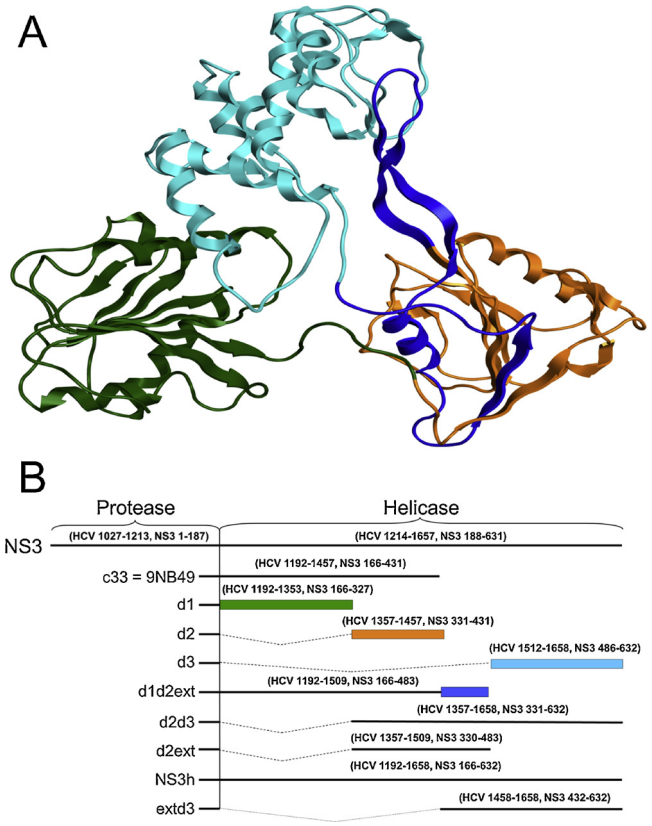

Fig. 1. (A) Ribbon diagram of a crystal structure of HCV NS3 helicase (PDB = 8OHM, (Cho et al., 1998)) displaying the triangular arrangement of domains, rendered using MOE software (Chemical Computing Group). (B) Series of domain addition/deletion variants constructed. Coloring of the ribbon diagram corresponds to coloring of domains as designated. Amino acid numbering is according to Kuiken (Kuiken et al., 2006).

2.2. 2-step indirect Chemiluminescent Magnetic Immunoassay (CMIA)

Evaluation of NS3 antibody reactivity was measured using the Abbott ARCHITECT®, a high throughput, fully automated analyzer that can be used to evaluate plasma or sera for antibodies and/or antigens associated with exposure to transfusion-transmitted viruses (Leary et al., 2006; Quinn, 2005). The ARCHITECT® HCV NS3 antibody research assays employed for this study (Fig. 2) consisted of a first step in which either human serum, human plasma, or mouse monoclonal anti-NS3 IgG samples were mixed with a sample diluent buffer, streptavidin-coated magnetic microparticles (Dynal M-270, Invitrogen) in suspension, and an NS3 recombinant protein possessing a carboxyl-terminal biotin tag (as described above). During an 18-min incubation step, antibodies directed against NS3, if present, were bound to the NS3 antigen, creating an immune complex which was then bound to streptavidin-coated magnetic microparticles via the biotin tag. After a wash step, the second assay step comprised addition of an acridinium-labeled anti-human or anti-mouse IgG monoclonal antibody (described below) to the reaction, followed by a 4-min incubation. After another wash step, a basic hydrogen peroxide solution was added to trigger a chemiluminescent reaction by the bound acridinium anti-human/mouse conjugate. The amount of light produced was measured and reported in relative light units (RLUs), proportional to the amount of antibody bound. Signal-to-noise ratio (S/N) was calculated as the ratio of RLUs (mean ± standard deviation of n = 3, unless otherwise specified) generated by the positive control or seroconversion sample to RLUs (mean ± standard deviation of n = 3, unless otherwise specified) generated by the negative control (described below). For seroconversion sensitivity testing, an S/N of 10.0 was used as a cutoff for positivity; hence, samples with S/N ≥ 10.0 were considered to be reactive, while samples with S/N < 10.0 were considered to be non-reactive.

2.3. Preparation of acridinium labeled conjugate

Monoclonal anti-human IgG was labeled directly with the *N*-hydroxysuccinimide (NHS) ester of 10-sulfopropyl-*n*-tosyl-*n*-(2-carboxyethyl)-9-acridinium carboxamide trifluoromethyl sulfonate at room temperature and then purified using size-exclusion chromatography and stored at 4 °C.

2.4. Human specimens—controls and seroconversion panels

For all immunoassays, a negative control sample was used that consisted of recalcified human plasma shown to be nonreactive for HBsAg, and negative for anti HCV, HIV-1 RNA or HIV-1 Ag, anti HIV 1/HIV-2 and anti-HTLV-I/HTLV-II. The anti-HCV NS3 reactive positive control (PC) was a recalcified human plasma sample reactive for a single anti-HCV marker as determined by Chiron RIBA HCV 3.0 SIA (2+ or greater c33 band intensity and nonreactive for other bands). The PC was diluted as needed in recalcified nonreactive human plasma, as described above. Commercially available human plasma (sodium citrate) seroconversion panels 6224, 6228, and 9044 were obtained from Zeptometrix (Franklin, MA) and panel 919 was obtained from SeraCare (Gaithersburg, MD).

3. Results

3.1. Seroreactivity of 9NB49H-Cbt and Cys → Ser mutants

The relative immunoreactivity of the 9NB49H recombinants and cysteine-to-serine substituted variants was measured in the presence or absence of 5 mM DTT, which was added to the microparticle suspension. Assays were performed as described in the Materials and Methods and in Fig. 2(A) using a known anti-HCV NS3 positive plasma pool (PC) and an HCV antibody negative normal human plasma. Results, expressed as sample/negative (S/N), are shown in Table 4. Seroreactivity of the singly substituted variants in the presence of DTT decreased in the order C4S > WT > C3S > > C5S > > C2S, suggesting that either or both C2 and C5 are involved in formation of critical c33 epitopes. C5 is not likely to be directly involved in formation of a critical epitope since the variant combining C4S with C5S retained 96.3% of wild-type 9NB49H seroreactivity. In contrast, each 9NB49H variant containing a C2S substitution (C2S, C1-3S, and C1-5S) retained < 32.2% of wild-type seroreactivity, suggesting that C2 is directly involved in formation of a critical c33 epitope. In the absence of DTT, both C3S and C4S showed enhanced seroreactivity, while each of the other variants showed some degree of compromised seroreactivity. Among the mutants that retained > 50% of 9NB49H seroreactivity, only C3S exhibited substantially diminished DTT-dependence,

Table 3
HCV NS3 helicase mutants evaluated. Position of codon (amino acid residues) mutated and resulting variant are given.

Position (s) in HCV polyprotein	Position (s) in NS3	NS3h designation	Rationale
K1236	K210	K46N	Eliminated ATPase activity (Tai et al., 2001)
S1237	S211	S47A	Coordinates Mg/Mn binding (Gu and Rice, 2010)
T1238	T212	T48E	Coordinates PO_4 binding (Gu and Rice, 2010)
Y1267	Y241	Y77S	Adenosine stacking residue (Gu and Rice, 2010)
D1316	D290	D126N	Eliminated ATPase activity (Tai et al., 2001)
E1317	E291	E127Q	Eliminated ATPase activity (Tai et al., 2001)
C1318	C292	C3S	Modify redox sensitivity, compromised helicase activity (Kim et al., 1997; Tai et al., 2001; Wardell et al., 1999)
H1319	H293	H129A	Compromised ATPase activity (Kim et al., 1997; Tai et al., 2001)
C1400	C374	C5S	Modify redox sensitivity
C1318 + C1400	C292 + C374	C3S + C5S	Modify redox sensitivity
P1256 + C1318 + C1400	P230 + C292 + C374	C3S + C5S + P66Q	Unintended, PCR error
T1445	T419	T255G	Coordinates adenosine binding (Gu and Rice, 2010)
Q1486	Q460	Q296H	Compromised ATPase activity (Kim et al., 1997; Tai et al., 2001; Wardell et al., 1999)
R1490	R464	R300A	Eliminated ATPase activity (Kim et al., 1997)
H1319 + R1490	H239A + R464	H129A + R300A	Unintended, PCR error
R1493	R467	R303K	Compromised ATPase activity (Kim et al., 1997; Wardell et al., 1999)
C1525	C499	C10S	Modify redox sensitivity
C1318 + C1525	C292 + C499	C3S + C10S	Modify redox sensitivity
W1527	W501	W337A	Eliminated helicase activity (Tai et al., 2001)
C1551	C525	C11S	Modify redox sensitivity
C1318 + C1551	C292 + C525	C3S + C11S	Modify redox sensitivity
C1648	C622	C14S	Modify redox sensitivity
C1318 + C1648	C292 + C622	C3S + C14S	Modify redox sensitivity

suggesting that C3 was not directly involved in a critical c33 epitope, but that oxidation of C3 in the wild-type was at least partially responsible for the observed redox sensitivity of the antigen.

To better evaluate the relative sensitivity of 9NB49H and the C3S variant for anti-HCV NS3 antibody detection, two human HCV seroconversion panels were evaluated with each of the capture antigens (Table 5). The 9NB49H-C3S-Cbt recombinant conferred greater assay sensitivity as evidenced by higher S/N values and by detection of 2 additional serial bleeds from the 6228 panel as compared to the wild-type.

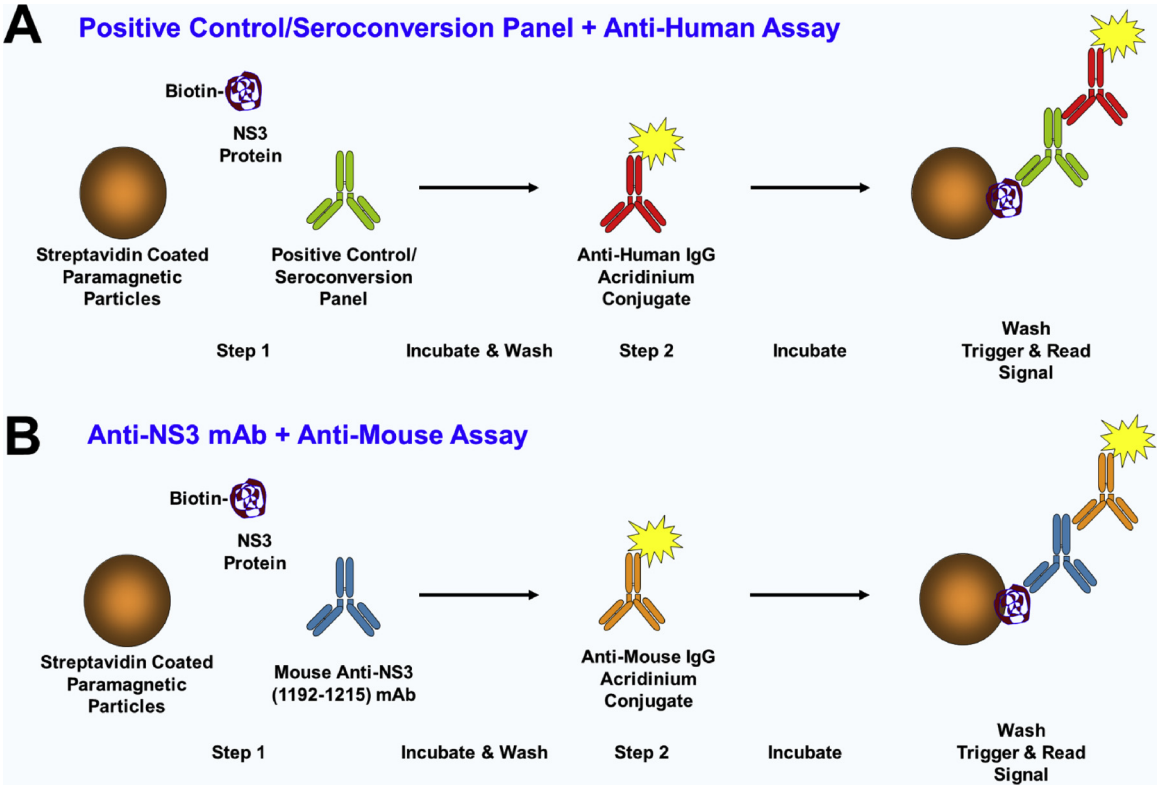

Fig. 2. 2-step Indirect Chemiluminescent Magnetic Immunoassay (CMIA) assay formats. (A) Seroreactivity of c33 and NS3h variants was assayed using either the anti-NS3 positive control plasma (PC) or seroconversion panels with anti-human IgG signal generating conjugate. (B) A second assay format used a well-characterized mouse monoclonal antibody with specificity for HCV NS3 amino acids 1192–1215, along with anti-mouse IgG signal generating conjugate in order to quantify the amount of NS3 antigen captured by the particles, thereby allowing normalization of the anti-NS3 positive control plasma signal across the series of ATPase/helicase variants.

Table 4
Relative seroreactivity of HCV NS3 Cys→Ser substituted variants in the presence/absence of 5 mM DTT.

9NB49H-Cbt protein	+ DTT		− DTT		% Change of S/N in the absence of DTT
	PC S/N	Relative to WT	PC S/N	Relative to WT	
9NB49H(WT)-Cbt	334.4 ± 31.7	–	206.0 ± 25.9	–	−38%
9NB49H(C1S)-Cbt	217.1 ± 20.5	64.9%	81.1 ± 1.9	39.3%	−63%
9NB49H(C2S)-Cbt	107.8 ± 8.4	32.2%	85.8 ± 8.2	41.7%	−20%
9NB49H(C3S)-Cbt	313.7 ± 31.7	93.8%	270.8 ± 32.3	131.5%	−14%
9NB49H(C4S)-Cbt	340.5 ± 23.2	101.8%	226.0 ± 16.6	109.7%	−34%
9NB49H(C5S)-Cbt	255.4 ± 18.1	76.4%	115.9 ± 62.0	56.3%	−55%
9NB49H(C1-3S)-Cbt	17.2 ± 2.0	5.1%	15.9 ± 1.7	7.7%	−8%
9NB49H(C4-5S)-Cbt	322.0 ± 25.1	96.3%	197.3 ± 17.9	95.8%	−39%
9NB49H(C1-5S)-Cbt	7.4 ± 0.8	2.2%	4.7 ± 0.6	2.3%	−37%

The % difference of PC S/N was calculated as: (PC S/N in the absence of reducing agent—PC S/N in the presence of reducing agent) × 100 (PC S/N in the presence of reducing agent).

Table 5
Anti-NS3 seroconversion sensitivity of 9NB49H-Cbt and the C3S variant thereof, in the presence of 5 mM DTT. Samples with S/N ≥ 10.0 are considered reactive.

	Bleed date	9NB49H-Cbt	9NB49 H(C3S)-Cbt	C3S:WT ratio
NC	N/A	1.0	1.0	–
PC	N/A	187.9	251.3	1.34
919-1	31-Dec-99	13.3	24.5	1.84
919-2	7-Jan-00	13.2	24.3	1.84
919-3	12-Jan-00	13.1	23.2	1.77
919-4	25-Jan-00	15.6	28.7	1.84
919-5	28-Jan-00	269.5	450.2	1.67
919-6	1-Feb-00	89.1	241.3	2.71
919-7	1-Apr-00	61.4	152.9	2.49
6228-1	20-Nov-96	1.0	0.7	0.70
6228-2	22-Nov-96	0.9	1.0	1.11
6228-3	27-Nov-96	1.1	0.8	0.73
6228-4	29-Nov-96	0.8	1.0	1.25
6228-5	4-Dec-96	0.8	0.7	0.88
6228-6	6-Dec-96	0.8	0.8	1.00
6228-7	11-Dec-96	0.9	0.8	0.89
6228-8	14-Dec-96	1.0	0.9	0.90
6228-9	18-Dec-96	6.2	12.3	1.98
6228-10	21-Dec-96	10.2	19.3	1.89
6228-11	26-Dec-96	9.2	16.3	1.77
6228-12	28-Dec-96	11.3	16.4	1.45

3.2. Seroreactivity of helicase domain addition/deletion variant series

To identify domains of the HCV NS3 helicase (NS3h) contributing to seroreactivity among HCV infected individuals, a series of recombinant proteins was made as shown in Fig. 1, and as detailed in Table 6. The NS3h(C3S) variant was included in this evaluation because of the promising results obtained in the previous study. Relative seroreactivity was determined using PC and a set of seroconversion panels from human individuals infected with HCV using the assay format shown in Fig. 2(A). An equimolar amount of NS3 recombinant protein was used for each assay. As shown in Table 6, NS3h(d2) and NS3h(d2ext) exhibited only 30% of the PC reactivity of 9NB49H, suggesting that critical c33 epitopes were either missing or were obscured by the antigen folding. NS3h(d1) was 30% more reactive than 9NB49H, suggesting that all critical c33 epitopes were contained within the helicase Domain 1 and that they were better exposed in the absence of Domain 2. Addition of the anti-parallel beta finger spanning the interface of domains 2 and 3 (Fig. 1A) had little effect as evidenced by the equivalent PC seroreactivity of 9NB49H and NS3h(d1d2ext). As had been demonstrated previously (Rebuzzini, 2009), full-length NS3 helicase was substantially more reactive than c33 (9NB49 H). The addition of domain 3 boosted seroreactivity of NS3h about 4.5-fold compared to 9NB49H, and NS3h(C3S) was about 6-fold more potent than 9NB49H in terms of PC seroreactivity.

Table 6
Relative seroreactivity of domain addition/deletion variants, in the presence of 5 mM DTT.

NS3h-Cbt domain variant	PC S/N	Fold difference vs. 9NB49H
9NB49H	5.7 ± 0.7	1.0
d1	7.5 ± 1.0	1.3
d2	1.7 ± 0.2	0.3
d2ext	1.7 ± 0.1	0.3
d1d2ext	5.6 ± 0.3	1.0
NS3h	25.9 ± 0.5	4.5
NS3h(C3S)	35.3 ± 2.2	6.1

In terms of seroconversion sensitivity (Table 7), 9NB49H and NS3h (d1d2ext) performed poorly as the capture reagent, detecting only a single positive among the 24 serial specimens evaluated across 3 panels, when a cutoff of ≥10 S/N was applied. Neither NS3h(d2) or NS3h

Table 7
Relative seroreactivity of NS3h and domain addition/deletion variants determined by seroconversion panel testing, in the presence of 5 mM DTT. S/N values are reported without associated error values because panel sample volume precluded repetitive testing. Samples with S/N ≥ 10.0 are considered reactive.

Panel member	Bleed date	NS3h-Cbt domain variant						
		9NB49H	d1	d2	d2ext	d1d2ext	NS3h	NS3h (C3S)
6224-01	28-Oct-96	0.9	0.9	0.9	0.8	0.8	0.9	1.0
6224-02	31-Oct-96	0.6	0.7	0.7	0.7	0.6	0.7	0.7
6224-03	4-Nov-96	0.7	0.7	0.7	0.7	0.7	1.9	2.4
6224-04	8-Nov-96	0.8	0.8	0.7	0.7	0.8	8.2	12.0
6224-05	16-Nov-96	2.8	4.9	0.7	0.7	3.3	24.6	33.0
6224-06	19-Nov-96	4.8	8.3	0.6	0.7	5.2	29.6	39.9
6228-01	20-Nov-96	0.9	1.0	1.0	1.0	1.0	1.0	0.9
6228-02	22-Nov-96	0.8	0.9	0.9	0.9	0.9	1.0	1.0
6228-03	27-Nov-96	1.0	1.0	1.0	1.0	1.0	1.1	1.0
6228-04	29-Nov-96	0.9	0.9	0.9	0.9	0.9	0.9	0.8
6228-05	4-Dec-96	1.0	1.0	1.1	1.1	1.1	1.1	1.0
6228-06	6-Dec-96	0.9	1.0	0.9	0.9	1.0	1.0	0.9
6228-07	11-Dec-96	1.0	1.1	1.0	1.0	1.1	1.4	1.5
6228-08	14-Dec-96	1.0	1.0	1.0	1.0	1.0	1.3	1.6
6228-09	18-Dec-96	1.9	3.2	1.1	1.1	1.9	8.4	12.9
6228-10	21-Dec-96	4.7	10.2	1.0	1.0	4.1	23.8	34.4
6228-11	26-Dec-96	6.2	15.2	1.2	1.1	6.1	31.9	42.4
6228-12	28-Dec-96	7.1	16.5	1.0	1.0	7.4	32.0	42.1
9044-01	14-Apr-97	1.8	1.8	1.8	1.8	1.9	1.9	1.8
9044-02	18-Apr-97	1.7	1.6	1.6	1.7	1.6	1.7	1.5
9044-03	1-May-97	1.7	1.9	1.9	1.8	1.9	2.0	2.1
9044-04	5-May-97	2.4	3.3	1.8	1.9	2.5	11.8	17.7
9044-05	9-May-97	6.3	13.9	n/a*	2.7	6.6	29.3	39.3
9044-06	13-May-97	11.5	22.4	3.0	3.3	14.0	36.3	49.7

* No result was returned for this sample.

(d2ext) detected a single positive specimen. Unexpectedly, NS3h(d1) outperformed 9NB49H, detecting 3 positives from panel 6228 compared to none for 9NB49H, and 2 positives from panel 9044 compared to only one for 9NB49H, which translated to earlier detection by 4 days. Both NS3h and NS3h(C3S) yielded substantially elevated S/N values and detected many more positive serial bleeds across all 3 panels, compared to 9NB49H. NS3h(C3S) detected the most serial positives (10 of 24) with the highest S/N values of any of the capture antigens. It was not possible to meaningfully quantify the shortening of the pre-seroconversion window with these antigens since 9NB49H failed to detect any bleeds from 2 of the 3 panels, but both NS3h and NS3h(C3S) detected anti-NS3 seroconversion 8 days prior to 9NB49H in panel 9044.

3.3. Seroreactivity of helicase/ATPase variant series

NS3h point mutants were evaluated using two assays where antigen captured by the streptavidin microparticle was reacted with PC or an anti-NS3 mouse monoclonal antibody directed against an amino-terminal linear epitope. The amount of anti-NS3 human antibody bound was determined using an acridinylated anti-Human IgG conjugate while an acridinylated goat anti-mouse polyclonal antibody was used for the anti-NS3 mouse monoclonal antibody. The ratio between the two assays provided a means for normalization of the human anti-NS3 immunoreactivity relative to the amount of NS3 recombinant antigen on the microparticle (Table 8). Each of the NS3h proteins exhibited higher reactivity for PC than did 9NB49H, and 14 of the 21 variants were more potent than wild-type NS3h (maximum of ~30%). This suggests that certain mutations involved in ATPase activity or ATP binding can enhance seroreactivity. The singly substituted NS3h(C14S) variant and the double mutant NS3h(C3S + C14S) were compromised in potency, exhibiting roughly half of the reactivity of the wild-type NS3h protein, though each was more potent than 9NB49H. This would indicate that the c33 epitope(s) were not perturbed by the C14S substitution, but that residue C14 formed part of an important NS3 helicase domain 3 epitope.

Table 8
Relative immunoreactivity of NS3h variants ranked by potency. Variants were assayed, in the presence of 5 mM DTT, using the formats shown in Fig. 2, from which potency was calculated as the ratio of reactivity to PC, using an anti-human conjugate, to reactivity to a mouse anti-NS3 monoclonal, using an anti-mouse conjugate. The reported values were normalized relative to the S/N obtained using either 9NB49H or NS3h (wild-type).

NS3-Cbt variant	Relative to 9NB49H	Relative to NS3h (WT)
C5S	3.07	1.31
E127Q	3.04	1.30
C11S	2.98	1.27
D126N	2.81	1.20
C3S + C5S	2.76	1.17
C3S + C5S + P66Q	2.75	1.17
R303K	2.71	1.16
H129A + R300A	2.69	1.15
C10S	2.66	1.13
S47A	2.58	1.10
C3S + C11S	2.56	1.09
R300A	2.52	1.07
T48E	2.49	1.06
Y77S	2.44	1.04
wild-type	2.35	1.00
T255G	2.28	0.97
K46N	2.27	0.97
H129A	2.23	0.95
W337A	2.23	0.95
C3S + C10S	2.17	0.93
C3S + C14S	1.36	0.58
C14S	1.21	0.52
9NB49H (c33)	1.00	0.43

4. Discussion

Most anti-HCV diagnostic assays utilize an NS3 recombinant antigen to capture human antibody. The goal of this study was to engineer a c33 for detection of NS3-specific anti-HCV antibodies to improve seroconversion sensitivity and shelf-life in an ARCHITECT® assay. Based on numerous published examples where HCV NS3 helicase was either refolded or expressed and purified in soluble form (19, 21, 22), an IPTG-inducible plasmid was constructed to enable low temperature induction. pET-9NB49H-Cbt, encoding a c33 antigen with C-terminal polyhistidine and biotin-incorporation tags, was expressed as a soluble protein in BL21(DE3) cells. Co-expression of biotin ligase via the pBirAcm plasmid for in-vivo site-specific biotin incorporation, enabled in-assay immobilization of the antigen on streptavidin coated paramagnetic particles. The indirect assay formats chosen for this study allowed many NS3 helicase variants to be tested in a rapid and consistent manner.

Three series of variants were designed and tested in iteration. The first was a series of cysteine-to-serine substituted mutants (Table 1), among which C3S exhibited improved PC seroreactivity in the absence of DTT and moderately enhanced seroconversion sensitivity compared to wild-type 9NB49H. C3, also known as C292 (NS3 numbering), is located within the highly conserved DECH motif, and has been thoroughly scrutinized for its role in modulating HCV NS3 ATPase activity (Kim et al., 1997; Tai et al., 2001; Wardell et al., 1999). In the ratchet mechanism of translocation, C3 is located within a highly dynamic region of the nucleotide-binding site (Gu and Rice, 2010). It is conceivable that replacement of cysteine with serine at this key position alters the protein conformation and accessibility of antibody-binding epitopes within c33.

9NB49H, representing c33, is comprised of helicase domains 1 and 2 (Fig. 1A), although the folding and arrangement of these domains outside the full-length helicase context are unknown. To evaluate the relative contributions of the three helicase structural domains and their interfaces, a second series of variants was constructed consisting of 8 additional proteins (Fig. 1B and Table 2), whereby the domains were expressed individually and in various combinations. With the exception of the full-length helicase (NS3h), any construct containing domain 3 failed to express in soluble form. Therefore, characterization of domain 3 seroreactivity in the absence of the other domains was not possible. Misfolding or aggregation of NS3h(d3)-Cbt, NS3h(d2d3)-Cbt, and NS3h (extd3)-Cbt suggested that formation of the interface between domains 1 and 3 may be required for proper folding of domain 3. Each of the other domain addition/deletion proteins was highly expressed, purified in monomeric form by a combination of IMAC and sizing, and subjected to seroreactivity evaluation (Tables 6 and 7). 9NB49H seroreactivity was not improved by extending the carboxyl terminus in the form of NS3h(d1d2ext). As anticipated, NS3h(d2) and NS3h(d2ext) were less reactive than 9NB49H with both PC and seroconversion samples due to the absence of critical epitopes within domain 1. We anticipated that NS3h(d1) would retain some fraction of the 9NB49H seroreactivity, but that deletion of the carboxyl-terminal half of the antigen would compromise critical domain 2 epitopes. To our surprise, NS3h(d1) exhibited improved PC reactivity and enabled improved seroconversion sensitivity, detecting 4 more serial bleeds than 9NB49H. These results led us to conclude that domain 2 contains few, if any, of the c33 epitopes, and that its removal permitted improved solvent accessibility of those within domain 1. Despite the improved performance of NS3h(d1) relative to 9NB49H, the full-length helicase proteins NS3h and NS3h(C3S) were much more potent. Enhanced seroreactivity of full-length NS3 helicase antigens was described previously (Rebuzzini, 2009). Taken together, these studies suggest that properly folded, soluble, and monomeric HCV NS3 helicase presents at least one conformational epitope from domain 3 that provides enhanced potency. This finding offers the potential to minimize the preseroconversion window inherent to anti-HCV antibody testing. We hypothesize that further gains in

seroreactivity may be realized by leveraging the conformational dynamics of the helicase enzyme to maximize epitope exposure.

Finally, a third series of full-length NS3 helicase variants was designed that consisted of single or paired substitutions at amino acids previously identified as important to ATPase/helicase catalysis (Table 3). This series included additional cysteine-to-serine variants based on the predicted solvent exposure of the thiol sidechain. Each of the mutants was expressed in soluble form, purified by IMAC, and characterized using the dual assay potency measurement. The potencies of the variant panel members are reported in Table 8. All 21 variants were more potent than 9NB49H, suggesting that these residues were not involved in c33 epitopes. Ten of the variants were at least 10% more potent than wild-type NS3h, suggesting that altering active site residues can indirectly influence epitope presentation. Since none of these variants had greater than 31% improvement in potency relative to NS3h, seroconversion sensitivity evaluation was not pursued. Cysteine-to-serine substitution of C14 (amino acid 622 by NS3 numbering) dramatically diminished the reactivity of NS3h, suggesting that this residue is involved in a key domain 3 epitope. The amino acid positions that were selected to be mutated in this series generally exhibited high degrees of sequence conservation, not only within each of the 7 well-characterized HCV genotypes (Smith et al., 2014), but across all HCV genotypes as well (see Supplemental Table S1). Due to the deleterious effects of these substitutions on enzymatic activity, it was not surprising that none of the variants we constructed were observed in nature. Nonetheless, it should be noted that a careful cross-genotype examination of assay sensitivity would be required before any such mutated NS3 helicase recombinant antigen could be used in a reliable anti-HCV serological test.

In this study, we have identified several promising HCV NS3 antigens that exhibit enhanced reactivity in comparison to c33. It is apparent that one or more of these proteins will improve the performance of an anti-HCV serological assay. Minimizing the preseroconversion window would be of benefit to individuals in regions where access to NAT testing is limited.

Disclaimer

The authors are employees of Abbott Laboratories.

Acknowledgments

We are grateful to Thomas Leary for critically reading the manuscript and to George Dawson and Suresh Desai for assistance with initial studies. Thanks also to Todd Meyer for helpful analysis of HCV sequence variation, and to Andrew Mathison, Mingyong Xiong, and Gerry Chan for useful discussion.

Appendix A. Supplementary data

Supplementary material related to this article can be found, in the online version, at doi:https://doi.org/10.1016/j.jviromet.2018.10.019.

References

Alter, H.J., Purcell, R.H., Shih, J.W., Melpolder, J.C., Houghton, M., Choo, Q.L., Kuo, G., 1989. Detection of antibody to hepatitis C virus in prospectively followed transfusion recipients with acute and chronic non-A, non-B hepatitis. N. Engl. J. Med. 321, 1494–1500.

Beckett, D., Kovaleva, E., Schatz, P.J., 1999. A minimal peptide substrate in biotin holoenzyme synthetase-catalyzed biotinylation. Protein Sci. 8, 921–929.

Cho, H.S., Ha, N.C., Kang, L.W., Chung, K.M., Back, S.H., Jang, S.K., Oh, B.H., 1998. Crystal structure of RNA helicase from genotype 1b hepatitis C virus. A feasible mechanism of unwinding duplex RNA. J. Biol. Chem. 273, 15045–15052.

Choo, Q.L., Kuo, G., Weiner, A.J., Overby, L.R., Bradley, D.W., Houghton, M., 1989. Isolation of a cDNA clone derived from a blood-borne non-A, non-B viral hepatitis genome. Science 244, 359–362.

Choo, Q.L., Weiner, A.J., Overby, L.R., Kuo, G., Houghton, M., Bradley, D.W., 1990. Hepatitis C virus: the major causative agent of viral non-A, non-B hepatitis. Br. Med. Bull. 46, 423–441.

Cloherty, G., Talal, A., Coller, K., Steinhart, C., Hackett Jr., J., Dawson, G., Rockstroh, J., Feld, J., 2016. Role of serologic and molecular diagnostic assays in identification and management of hepatitis C virus infection. J. Clin. Microbiol. 54, 265–273.

Gibson, D.G., Young, L., Chuang, R.Y., Venter, J.C., Hutchison 3rd., C.A., Smith, H.O., 2009. Enzymatic assembly of DNA molecules up to several hundred kilobases. Nat. Methods 6, 343–345.

Gu, M., Rice, C.M., 2010. Three conformational snapshots of the hepatitis C virus NS3 helicase reveal a ratchet translocation mechanism. Proc. Natl. Acad. Sci. U. S. A. 107, 521–528.

Kim, D.W., Kim, J., Gwack, Y., Han, J.H., Choe, J., 1997. Mutational analysis of the hepatitis C virus RNA helicase. J. Virol. 71, 9400–9409.

Kleinman, S., Alter, H., Busch, M., Holland, P., Tegtmeier, G., Nelles, M., Lee, S., Page, E., Wilber, J., Polito, A., 1992. Increased detection of hepatitis C virus (HCV)-infected blood donors by a multiple-antigen HCV enzyme immunoassay. Transfusion 32, 805–813.

Kuiken, C., Mizokami, M., Deleage, G., Yusim, K., Penin, F., Shin, I.T., Charavay, C., Tao, N., Crisan, D., Grando, D., Dalwani, A., Geourjon, C., Agrawal, A., Combet, C., 2006. Hepatitis C databases, principles and utility to researchers. Hepatology 43, 1157–1165.

Kuo, G., Choo, Q.L., Alter, H.J., Gitnick, G.L., Redeker, A.G., Purcell, R.H., Miyamura, T., Dienstag, J.L., Alter, M.J., Stevens, C.E., et al., 1989. An assay for circulating antibodies to a major etiologic virus of human non-A, non-B hepatitis. Science 244, 362–364.

Leary, T.P., Gutierrez, R.A., Muerhoff, A.S., Birkenmeyer, L.G., Desai, S.M., Dawson, G.J., 2006. A chemiluminescent, magnetic particle-based immunoassay for the detection of hepatitis C virus core antigen in human serum or plasma. J. Med. Virol. 78, 1436–1440.

Lee, S.R., Wood, C.L., Lane, M.J., Francis, B., Gust, C., Higgs, C.M., Nelles, M.J., Polito, A., DiNello, R., Achord, D., 1995. Increased detection of hepatitis C virus infection in commercial plasma donors by a third-generation screening assay. Transfusion 35, 845–849.

Lelie, P.N., Cuypers, H.T., Reesink, H.W., van der Poel, C.L., Winkel, I., Bakker, E., van Exel-Oehlers, P.J., Vallari, D., Allain, J.P., Mimms, L., 1992. Patterns of serological markers in transfusion-transmitted hepatitis C virus infection using second-generation HCV assays. J. Med. Virol. 37, 203–209.

Ogata, N., Alter, H.J., Miller, R.H., Purcell, R.H., 1991. Nucleotide sequence and mutation rate of the H strain of hepatitis C virus. Proc. Natl. Acad. Sci. U. S. A. 88, 3392–3396.

Palenzuela, D.O., Pedroso, S., Roca, J., Villareal, A., Lemos, G., Reyes, O., Novoa, L., 2006. A new NS3 recombinant protein shows improved antigenic properties for HCV diagnosis. Biotechnol. Appl. 23, 94–98.

Quinn, F.A., 2005. Bulk reagent random-access analyzers: ARCHITECT i2000Reg and i2000SR analyzers. In: Wild, D. (Ed.), The Immunoassay Handbook, 3rd edition. Elsevier Science.

Rebuzzini, G., 2009. Study of the Hepatitis C Virus NS3 Helicase Domain for Application in a Chemiluminescent Immunoassay, Facoltà di Scienze Matematiche, Fisiche e Naturali Dipartimento di Biotecnologie e Bioscienze. Universita Degli Studi Di Milano, Bicocca, pp. 1–95.

Selvarajah, S., Busch, M.P., 2012. Transfusion transmission of HCV, a long but successful road map to safety. Antivir. Ther. (Lond.) 17, 1423–1429.

Smith, D.B., Bukh, J., Kuiken, C., Muerhoff, A.S., Rice, C.M., Stapleton, J.T., Simmonds, P., 2014. Expanded classification of hepatitis C virus into 7 genotypes and 67 subtypes: updated criteria and genotype assignment web resource. Hepatology 59, 318–327.

Tai, C.L., Pan, W.C., Liaw, S.H., Yang, U.C., Hwang, L.H., Chen, D.S., 2001. Structure-based mutational analysis of the hepatitis C virus NS3 helicase. J. Virol. 75, 8289–8297.

UniProt, C., 2015. UniProt: a hub for protein information. Nucleic Acids Res. 43, D204–D212.

Wardell, A.D., Errington, W., Ciaramella, G., Merson, J., McGarvey, M.J., 1999. Characterization and mutational analysis of the helicase and NTPase activities of hepatitis C virus full-length NS3 protein. J. Gen. Virol. 80 (Pt 3), 701–709.

Wise, M., Bialek, S., Finelli, L., Bell, B.P., Sorvillo, F., 2008. Changing trends in hepatitis C-related mortality in the United States, 1995–2004. Hepatology 47, 1128–1135.